CSIRO PUBLISHING

RESEARCH FRONT

Aust. J. Chem. **2013**, *66*, 1211–1218
http://dx.doi.org/10.1071/CH13106

Full Paper

Synthesis and Reactivity of Half-Sandwich Ruthenium κ^2-Aminoborane Complexes

David A. Addy,[A] *Joshua I. Bates,*[A] *Michael J. Kelly,*[A] *Joseph Abdalla,*[A] *Nicholas Phillips,*[A] *Ian M. Riddlestone,*[A] *and Simon Aldridge*[A,B]

[A]Inorganic Chemistry Laboratory, Department of Chemistry, University of Oxford, South Parks Road, Oxford, OX1 3QR, UK.
[B]Corresponding author. Email: Simon.Aldridge@chem.ox.ac.uk

Cationic half-sandwich ruthenium complexes featuring κ^2-bound aminoborane ligands can readily be accessed from 16-electron precursors via chloride abstraction in the presence of H_2BNR_2 (R = ^{i}Pr, Cy). Complexes [Cp*Ru(L)(κ^2-H_2BNR_2)][BAr$^f_4$] (**2a**: R = ^{i}Pr, L = PCy_3; **2b**: R = ^{i}Pr, L = PPh_3; **2c**: R = ^{i}Pr, L = 1,3-bis-(2,4,6-trimethylphenyl)-imidazol-2-ylidene; **3a**: R = Cy, L = PCy_3; Ar^f = $C_6H_3(CF_3)_2$-3,5) were isolated in yields of ~60 %, and characterised in the solid state by X-ray crystallography (for **2a**, **2c**, and **3a**). Low-field ^{11}B NMR shifts for the coordinated aminoborane fragment, together with short Ru···B contacts (of the order of 1.97 Å) imply a relatively tightly bound borane ligand, a finding which is given further credence by the results of density functional theory studies (e.g. bond dissociation energies in the range 24 kcal mol^{-1}; 1 kcal mol^{-1} = 4.186 kJ mol^{-1}). In terms of reactivity, κ^2 systems of this type, while potentially offering a versatile route to asymmetric κ^1 systems, in fact undergo borane extrusion even in the presence of a single equivalent of added ligand.

Manuscript received: 5 March 2013.
Manuscript accepted: 27 May 2013.
Published online: 27 June 2013.

Introduction

Aminoboranes, H_2BNRR' have been the focus of considerable recent research effort. This reflects not only their potential relevance to energy storage applications as the products of dehydrogenation of high hydrogen content BN-containing materials, but also as the monomeric building blocks from which a class of novel inorganic polymer can be assembled.[1,2] Despite their isoelectronic relationship with alkenes, however, and the wealth of metal complexes known for C=C double bonds, the coordination chemistry of aminoboranes is more limited, being restricted to a dozen or so structurally characterised examples.[3–6] Typically such complexes feature chelating H_2BNR_2 ligands coordinated to $[L_2M(H)_2]^{n+}$ fragments via two B-H-M bridges (M = Ru, n = 0; M = Rh, Ir, n = 1; L = N-heterocyclic carbene, tertiary phosphine) and are formed either by the direct coordination of an aminoborane or by the in situ dehydrogenation of the corresponding amine-borane, $H_3B{\cdot}NR_2H$.[3–6] Thus, for example, in earlier reports we have characterised κ^2 σ-complexes of aminoboranes at Group 9 metal centres featuring N-heterocyclic carbene co-ligands generated by the in situ dehydrogenation of $H_3B{\cdot}NR_2H$ (R = Me, ^{i}Pr, Cy) (Scheme 1).[5b,d,h,i] Related charge neutral ruthenium aminoborane complexes such as Ru(PCy_3)$_2$(H)$_2$(κ^2-$H_2BN^iPr_2$) have been prepared by Weller, Alcaraz, and Sabo-Etienne either via an analogous dehydrogenation approach or by the direct reaction of an aminoborane with a ruthenium *bis*(dihydrogen) complex.[5a,e,f,g] Moreover, reports from both Sabo-Etienne and Stradiotto confirm that such a coordination mode is not confined to aminoboranes, with a similar motif having been established for the more electrophilic mesitylborane, H_2BMes.[7–9] Thus, the reaction of Cp*Ru(P^iPr_3)Cl with $(H_2BMes)_n$ followed by halide abstraction yields a κ^2 borane complex featuring the 14-electron $[Cp^*Ru(P^iPr_3)]^+$ fragment.[8] With this in mind, we postulated that similar chemistry applied to the monomeric secondary aminoboranes H_2BNR_2 (R = ^{i}Pr or Cy) might provide access to half sandwich aminoborane complexes of the type $[Cp^*Ru(L)(\kappa^2\text{-}H_2BNR_2)]^+$. Such systems might provide an instructive comparison – both in terms of structural and reaction chemistry - with related κ^1-complexes of the type $[Cp^*Ru(L)_2(\kappa^1\text{-}H_2BNR_2)]^+$ recently developed in our program.[6]

Experimental

General

Manipulation of air-sensitive reagents was carried out in a glove-box, or by means of Schlenk-type techniques involving the use of a dry argon or nitrogen atmosphere. With the exception of fluorobenzene which was distilled from CaH_2, HPLC grade solvents were purified, dried, and degassed before use by a commercial Braun Solvent Purification System (SPS 500). [D_2]dichloromethane was pre-dried over molecular sieves before use. The known compounds H_2BNR_2 (R = ^{i}Pr, Cy), Cp*Ru(L)Cl (L = PCy_3, PPh_3, IMes = 1,3-bis-(2,4,6-trimethylphenyl)-imidazol-2-ylidene) and Na[BAr$^f_4$] [where Ar^f = $C_6H_3(CF_3)_2$-3,5] were prepared according to literature procedures[10]; ^{t}BuNC was used as supplied (Sigma Aldrich). Spectroscopic data for compound [**2a**][BAr$^f_4$] were included in a preliminary communication.[6b] ^{1}H and ^{13}C NMR spectra were measured on a Bruker AVII 500 FT-NMR or Varian Mercury

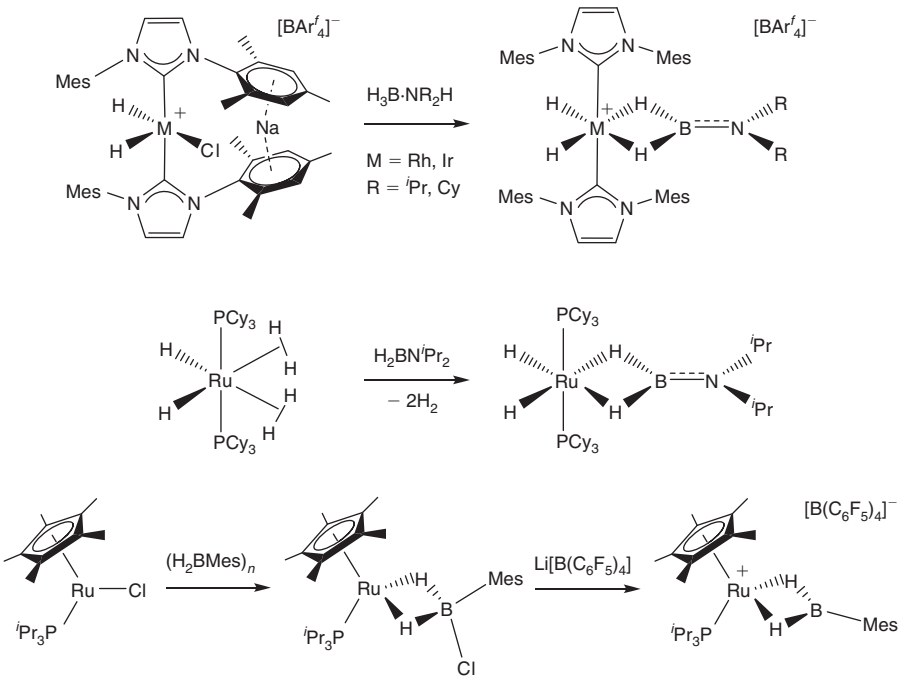

Scheme 1. Previous reports of κ^2 borane coordination of primary relevance to the current study.

VX-300 spectrometer, at 25°C, and calibrated using the residual proton or natural abundance ^{13}C resonances of the solvent; ^{11}B and ^{19}F spectra were referenced with respect to $Et_2O{\cdot}BF_3$ and $CFCl_3$, respectively. Mass spectra were measured by the EPSRC National Mass Spectrometry Service, Swansea University or in-house using a Bruker MicroToF instrument linked to an inert atmosphere dry box for sample injection. Elemental microanalyses were carried out at London Metropolitan University.

Syntheses of New Compounds

*[Cp*Ru(L)(κ^2-H$_2$BNR$_2$)][BAr$^f_4$], [**2a**–**c**][BAr$^f_4$] and [**3a**][BAr$^f_4$]*

The four compounds were prepared by a common method, exemplified here for [**3a**][BAr$^f_4$]. H_2BNCy_2 (0.37 cm^3 of a 0.29 M solution in C_6H_5F, 0.11 mmol) was added to a solution of Cp*Ru(PCy$_3$)Cl (0.03 g, 0.05 mmol) in fluorobenzene (~0.7 mL). The blue reaction mixture was then added to Na[BAr$^f_4$] (0.05 g, 0.06 mmol) and an instant colour change to yellow was observed. The solution was filtered, layered with hexanes (30 mL) and red crystals suitable for X-ray crystallography were obtained in 65 % yield. [**2a**–**c**][BAr$^f_4$] were prepared in analogous fashion from $H_2BN^iPr_2$ and Cp*Ru(L)Cl (**1a**: L = PCy$_3$; **1b**: L = PPh$_3$; **1c**: L = IMes) in yields of ~60, 50, and 60 %, respectively.

Data for [**3a**][BAr$^f_4$]: ^{1}H NMR (300 MHz, [D$_2$]dichloromethane): δ_H −11.22 (br s, 2H, RuBH), 0.97–2.16 (overlapping m, 53H, CH and CH$_2$ of PCy$_3$, CH$_2$ of NCy$_2$), 1.78 (s, 15H, CH$_3$ of Cp*), 2.89 (m, 2H, CH of NCy$_2$), 7.46 (s, 4H, *para*-CH of [BAr$^f_4$]$^-$), 7.63 (s, 8H, *ortho*-CH of [BAr$^f_4$]$^-$); ^{13}C NMR (126 MHz, [D$_2$]dichloromethane): δ_C 11.9 (CH$_3$ of Cp*), 25.6 (NCy$_2$ CH$_2$-4), 26.5 (NCy$_2$ CH$_2$-3), 26.7 (PCy$_3$ CH$_2$-4), 27.9 (d, $^2J_{PC}$ = 10.3 Hz, PCy$_3$ CH$_2$-2), 30.3 (NCy$_2$ CH$_2$-2), 36.0 (d, $^3J_{CP}$ = 2.7 Hz, PCy$_3$ CH$_2$-3), 37.6 (d, $^1J_{CP}$ = 20.7 Hz, PCy$_3$ CH), 58.9 (NCy$_2$ CH-1), 95.3 (Cp*), 117.9 (*para*-CH of [BAr$^f_4$]$^-$), 125.0 (q, $^1J_{CF.}$ = 274.0 Hz, CF$_3$ of [BAr$^f_4$]$^-$), 129.3 (q, $^2J_{CF.}$ = 31.0 Hz, *meta*-quaternary C of [BAr$^f_4$]$^-$), 135.1 (*ortho*-CH of [BAr$^f_4$]$^-$), 162.1 (q, $^1J_{CB}$ = 50.1 Hz, *ipso*-quaternary C of [BAr$^f_4$]$^-$); ^{11}B NMR (96 MHz, [D$_2$]dichloromethane): δ_B 56.5 (br s, fwhm = 300 Hz, H_2BNCy_2), −6.1 ([BAr$^f_4$]$^-$); ^{19}F NMR (282 MHz, [D$_2$]dichloromethane): δ_F −62.0 (CF$_3$); ^{31}P{^{1}H} NMR (121 MHz, [D$_2$]dichloromethane): δ_P 54.4; *m/z* (ESI+) 710.5 (100 %, [M]$^{+\bullet}$); Found: C 54.93, H 5.40, N 0.89 %; M$^{+\bullet}$, 710.4505. $C_{72}H_{85}B_2F_{24}NPRu$ requires C 55.18, H 5.32, N 0.73 %; M$^{+\bullet}$, 710.4550.

Data for [**2a**][BAr$^f_4$]: ^{1}H NMR (300 MHz, [D$_2$]dichloromethane): δ_H −11.21 (br s, 2H, RuBH), 1.11–1.87 (m, 33H, PCy$_3$), 1.22 (d, $^3J_{HH}$ = 6.6 Hz, 12H, CH$_3$ of ^{i}Pr), 1.81 (s, 15H, CH$_3$ of Cp*), 3.39 (sept, $^3J_{HH}$ = 6.6 Hz, 2H, CH of ^{i}Pr), 7.47 (s, 4H, *para*-CH of [BAr$^f_4$]$^-$), 7.64 (s, 8H, *ortho*-CH of [BAr$^f_4$]$^-$); ^{13}C NMR (126 MHz, [D$_2$]dichloromethane): δ_C 11.9 (CH$_3$ of Cp*), 24.7, 26.7 (Cy CH$_2$-3,4), 27.9 (d, $^2J_{PC}$ = 10.1 Hz, Cy CH$_2$-2), 30.3 (CH$_3$ of ^{i}Pr), 37.7 (d, $^1J_{PC}$ = 21.1 Hz, Cy CH), 49.9 (CH of ^{i}Pr), 95.3 (Cp*), 117.9 (*para*-CH of [BAr$^f_4$]$^-$), 125.0 (q, $^1J_{CF.}$ = 274.0 Hz, CF$_3$ of [BAr$^f_4$]$^-$), 129.3 (q, $^2J_{CF.}$ = 31.0 Hz, *meta*-quaternary C of [BAr$^f_4$]$^-$), 135.1 (*ortho*-CH of [BAr$^f_4$]$^-$), 162.1 (q, $^1J_{CB}$ = 50.1 Hz, *ipso*-quaternary C of [BAr$^f_4$]$^-$); ^{11}B NMR (96 MHz, [D$_2$]dichloromethane): δ_B 56.2 (br s, fwhm = 300 Hz, $H_2BN^iPr_2$), −6.1 ([BAr$^f_4$]$^-$); ^{19}F NMR (282 MHz, [D$_2$]dichloromethane): δ_F −62.0 (CF$_3$); ^{31}P{^{1}H} NMR (121 MHz, [D$_2$]dichloromethane): δ_P 53.3; *m/z* (ESI+) 630.4 (100 %, [M]$^{+\bullet}$); Found: C 52.87, H 4.92, N 0.86 %; M$^{+\bullet}$, 630.3980. $C_{66}H_{76}B_2F_{24}NPRu$ requires C 53.08, H 5.09, N 0.94 %; M$^{+\bullet}$, 630.3922.

Data for [**2b**][BAr$^f_4$]: ^{1}H NMR (300 MHz, [D$_2$]dichloromethane): δ_H −10.45 (br s, 2H, RuBH), 1.47 (d, $^3J_{HH}$ = 6.6 Hz, 12H, CH$_3$ of ^{i}Pr), 1.56 (s, 15H, CH$_3$ of Cp*), 3.04 (sept, $^3J_{HH}$ = 6.6 Hz, 2H, CH of ^{i}Pr), 7.48 (s, 4H, *para*-CH of [BAr$^f_4$]$^-$), 7.34–7.66 (overlapping m, 15H, PPh$_3$), 7.64 (s, 8H, *ortho*-CH of [BAr$^f_4$]$^-$); ^{13}C NMR (126 MHz, [D$_2$]dichloromethane): δ_C 10.8 (CH$_3$ of Cp*), 32.0 (CH$_3$ of ^{i}Pr), 50.6 (CH of ^{i}Pr), 97.7 (Cp*), 117.9 (*para*-CH of [BAr$^f_4$]$^-$), 125.0 (q, $^1J_{CF.}$ = 274.0 Hz, CF$_3$ of [BAr$^f_4$]$^-$), 129.3 (q, $^2J_{CF.}$ = 31.0 Hz, *meta*-quaternary C of [BAr$^f_4$]$^-$), 130.3 (d, $^4J_{CP}$ = 10.5 Hz, *para*-CH of Ph), 133.7 (d, $^3J_{CP}$ = 11.7 Hz, *meta*-CH of Ph), 134.4

(d, $^2J_{CP}$ = 12.3 Hz, *ortho*-CH of Ph), 134.8 (d, $^1J_{CP}$ = 50.0 Hz, *ipso*-C of Ph), 135.1 (*ortho*-CH of [BAr$^f_4$]$^-$), 162.1 (q, $^1J_{CB}$ = 50.1 Hz, *ipso*-quaternary C of [BAr$^f_4$]$^-$); ^{11}B NMR (96 MHz, [D$_2$]dichloromethane): δ_B 57.2 (br s, fwhm = 380 Hz, H$_2$BN^{i}Pr$_2$), −6.1 ([BAr$^f_4$]$^-$); ^{19}F NMR (282 MHz, [D$_2$]dichloromethane): δ_F −62.8 (CF$_3$); ^{31}P{^{1}H} NMR (121 MHz, [D$_2$] dichloromethane): δ_P 50.5; *m/z* (ESI+) 612.2 ([M]$^{+\bullet}$); *m/z* (HR-MS) 612.2454; [M]$^+$ requires 612.2513; The fact that this compound is an oil prevented its isolation at a level of purity suitable for elemental microanalysis.

Data for [**2c**][BAr$^f_4$]: ^{1}H NMR (300 MHz, [D$_2$]dichloromethane): δ_H −9.71 (br s, 2H, RuBH), 1.10 (d, $^3J_{HH}$ = 6.6 Hz, 12H, CH$_3$ of ^{i}Pr), 1.35 (s, 15H, CH$_3$ of Cp*), 1.98 (br s, 12H, *ortho*-CH$_3$ of Mes), 2.27 (s, 6H, *para*-CH$_3$ of Mes), 3.14 (sept, $^3J_{HH}$ = 6.6 Hz, 2H, CH of ^{i}Pr), 6.97 (s, 4H, *meta*-CH of Mes), 7.04 (s, 2H, NCH of IMes), 7.48 (s, 4H, *para*-CH of [BAr$^f_4$]$^-$), 7.64 (s, 8H, *ortho*-CH of [BAr$^f_4$]$^-$); ^{13}C NMR (126 MHz, [D$_2$] dichloromethane): δ_C 11.0 (CH$_3$ of Cp*), 19.6 (*para*-CH$_3$ of Mes), 20.2 (*ortho*-CH$_3$ of Mes), 21.1 (CH$_3$ of ^{i}Pr), 49.4 (CH of ^{i}Pr), 91.7 (Cp*), 117.9 (*para*-CH of [BAr$^f_4$]$^-$), 124.9 (q, $^1J_{CF.}$ = 273.0 Hz, CF$_3$ of [BAr$^f_4$]$^-$), 125.6 (NCH of IMes), 129.2 (q, $^2J_{CF.}$ = 32.0 Hz, *meta*-quaternary C of [BAr$^f_4$]$^-$), 130.0 (*ortho*-C of Mes), 135.2 (*meta*-C of Mes), 137.3 (*para*-C of Mes), 140.1 (*ipso*-C of Mes), 135.1 (*ortho*-CH of [BAr$^f_4$]$^-$), 162.2 (q, $^1J_{CB}$ = 50.1 Hz, *ipso*-quaternary C of [BAr$^f_4$]$^-$), 180.2 (carbene quaternary-C of IMes); ^{11}B NMR (96 MHz, [D$_2$] dichloromethane): δ_B 49.9 (br s, fwhm = 340 Hz, H$_2$BN^{i}Pr$_2$), −6.1 ([BAr$^f_4$]$^-$); ^{19}F NMR (282 MHz, [D$_2$]dichloromethane): δ_F −62.8 (CF$_3$); *m/z* (ESI+) 654.4 (100 %, [M]$^{+\bullet}$); Found: C 54.76, H 4.27, N 2.65 %; M$^{+\bullet}$, 654.3542. C$_{69}$H$_{67}$B$_2$F$_{24}$N$_3$Ru requires C 54.61, H 4.45, N 2.77 %; M$^{+\bullet}$, 654.3542.

*[Cp*Ru(PCy$_3$)(CN^{t}Bu)$_2$)][BAr$^f_4$], [**4a**][BAr$^f_4$]*

A solution of [**2a**][BAr$^f_4$] (0.020 g, 0.013 mmol) in fluorobenzene (~0.7 mL) was added to a solution of ^{t}BuNC (0.034 mL, 0.030 mmol) also in fluorobenzene (~0.7 mL) and the reaction mixture was sonicated for 5 min. In situ monitoring by ^{11}B NMR spectroscopy revealed the generation of free H$_2$BN^{i}Pr$_2$ at this point (δ_B = 35.4, t, $^1J_{BH}$ = 126 Hz). Filtration and layering with hexanes (30 mL) led to the formation of yellow crystals suitable for X-ray crystallography in 60 % yield.

Data for [**4a**][BAr$^f_4$]: ^{1}H NMR (300 MHz, [D$_2$]dichloromethane): δ_H 1.10–1.90 (m, 33H, PCy$_3$), 1.36 (s, 18H, ^{t}BuNC), 1.73 (s, Cp*), 7.48 (s, 4H, *para*-CH of [BAr$^f_4$]$^-$), 7.64 (s, 8H, *ortho*-CH of [BAr$^f_4$]$^-$); ^{13}C NMR (126 MHz, [D$_2$]dichloromethane): δ_C 10.8 (CH$_3$ of Cp*), 26.6 (Cy CH$_2$-4), 27.8 (d, $^2J_{PC}$ = 10.4 Hz, Cy CH$_2$-2), 30.6 (Cy CH$_2$-3), 31.0 (CH$_3$ of ^{t}BuNC), 37.4 (d, $^1J_{PC}$ = 20.0 Hz, Cy CH-1), 57.9 (^{t}Bu quaternary-C of ^{t}BuNC), 96.3 (Cp*), 117.9 (*para*-CH of [BAr$^f_4$]$^-$), 125.0 (q, $^1J_{CF.}$ = 274.0 Hz, CF$_3$ of [BAr$^f_4$]$^-$), 129.3 (q, $^2J_{CF.}$ = 31.0 Hz, *meta*-quaternary C of [BAr$^f_4$]$^-$), 135.1 (*ortho*-CH of [BAr$^f_4$]$^-$), 153.7 (CN of ^{t}BuNC), 162.1 (q, ^{1}J$_{CB}$ = 50.1 Hz, *ipso*-quaternary C of [BAr$^f_4$]$^-$); ^{19}F NMR (282 MHz, [D$_2$]dichloromethane): δ_F −62.0 (CF$_3$); ^{31}P{^{1}H} NMR (121 MHz, [D$_2$]dichloromethane): δ_P 57.4; *m/z* (ESI+) 683.4 (100 %, [M]$^{+\bullet}$); *m/z* (HR-MS) 683.4011; [M]$^+$ requires 683.4012.

Crystallographic Method

With the exception of **4a**, data were collected on a NoniusKappa CCD diffractometer (Mo-Kα radiation, λ = 0.71073 Å) at 150 K. Data for **4a** were collected on an Oxford Diffraction Supernova diffractometer (Cu-Kα radiation, λ = 1.54180 Å) at 150 K. Data were processed using either the *DENZO-SMN* package or *CrysAlis*, and structures solved using *SIR92*. Refinement was carried out using full-matrix least-squares within the *CRYSTALS* suite.[11] Full crystallographic data for all structures have been deposited with the Cambridge Crystallographic Data Centre, CCDC references 909183 and 927354–927356. Copies of these data can be obtained free of charge from The Cambridge Crystallographic Data Centre via www.ccdc.cam.ac.uk/data_request/cif.

[**2a**][BAr$^f_4$]: C$_{66}$H$_{76}$B$_2$F$_{24}$NPRu, M$_w$ = 1492.95, monoclinic, P2$_1$/c, *a* = 19.2398(1), *b* = 14.1958(1), *c* = 25.3427(2) Å, β = 99.7258(3)°, V = 3157.5(4) Å^3, Z = 4, ρ$_c$ = 1.453 Mg m^{-3}, *t* = 150 K, λ = 0.71073 Å. 185601 reflections collected, 15523 independent [R(int) = 0.025] and used in all calculations. R$_1$ = 0.0428, *w*R$_2$ = 0.1011 for observed unique reflections [F^2 >2σ (F^2)] and R$_1$ = 0.0660, *w*R$_2$ = 0.1119 for all unique reflections. Max. and min. residual electron densities 0.93 and −0.82 e Å^{-3}. CCDC reference: 909183.

[**2c**][BAr$^f_4$]: C$_{69}$H$_{67}$B$_2$F$_{24}$N$_3$Ru, M$_w$ = 1517.42, triclinic, P-1, *a* = 12.8454(3), *b* = 15.9928(4), *c* = 18.3511(5) Å, α = 78.7012(10)°, β = 76.2493(11)°, γ = 77.1539(10)°, V = 3529.3(2) Å^3, Z = 2, ρ$_c$ = 1.425 Mg m^{-3}, *t* = 150 K, λ = 0.71073 Å. 20604 reflections collected, 12713 independent [R(int) = 0.038] and used in all calculations. R$_1$ = 0.0729, *w*R$_2$ = 0.1832 for observed unique reflections [F^2 >2σ (F^2)] and R$_1$ = 0.1003, *w*R$_2$ = 0.02081 for all unique reflections. Max. and min. residual electron densities 1.45 and −1.18 e Å^{-3}. CCDC reference: 927354.

[**3a**][BAr$^f_4$]: C$_{72}$H$_{85}$B$_2$F$_{24}$NPRu, M$_r$ = 1573.08, monoclinic, P2$_1$, *a* = 12.7773(1), *b* = 17.3289(1), *c* = 17.9242(1) Å, β = 98.4578(3)°, V = 3925.55(4) Å^3, Z = 2, ρ$_c$ = 1.331 Mg m^{-3}, *t* = 150 K, λ = 0.71073 Å. 69624 reflections collected, 16317 independent [R(int) = 0.045] and used in all calculations. R$_1$ = 0.0503, *w*R$_2$ = 0.1134 for observed unique reflections [F^2 >2σ (F^2)] and R$_1$ = 0.0453, *w*R$_2$ = 0.1083 for all unique reflections. Max. and min. residual electron densities 0.95 and −0.49 e Å^{-3}. CCDC reference: 927355.

[**4a**][BAr$^f_4$]: C$_{70}$H$_{78}$BF$_{24}$N$_2$PRu, M$_w$ = 1546.23, monoclinic, P2$_1$/c, *a* = 13.7490(1), *b* = 19.5577(2), *c* = 27.5241(2) Å, β = 99.970(1)°, V = 7400.1(1) Å^3, Z = 4, ρ$_c$ = 1.388 Mg m^{-3}, *t* = 150 K, λ = 1.54180 Å. 46253 reflections collected, 15366 independent [R(int) = 0.027] and used in all calculations. R$_1$ = 0.0681, *w*R$_2$ = 0.1718 for observed unique reflections [F^2 >2σ (F^2)] and R$_1$ = 0.0743, *w*R$_2$ = 0.1810 for all unique reflections. Max. and min. residual electron densities 1.71 and −1.04 e Å^{-3}. CCDC reference: 927356.

Computational Method

Density functional theory (DFT) calculations were performed using the Amsterdam Density Functional (ADF) Package Software 2012.[12a–c] Calculations were performed using the Vosko-Wilk-Nusair local density approximation with exchange from Becke,[12d] and correlation corrections from Perdew (BP).[12e] Slater-type orbitals (STOs) were used for the triple zeta basis set with an additional set of polarisation functions (TZP).[12f] The large frozen core basis set approximation was applied with no molecular symmetry, and the general numerical integration was six. Frequency calculations were performed for all freely optimised species and no significant imaginary frequencies were observed. Estimates of binding energies were obtained following the strategy outlined by Baerends,[12g] using the counterpoise method.[12h] Given that basis set superposition errors (BSSE) tend to be overestimated

by the counterpoise method,[12i] and that the BSSE for $[\mathbf{2a}]^+$ and model versions were found to be less than 2 kcal mol^{-1}, reaction energies are discussed without BSSE correction. Bonding analyses employed a combined charge and energy decomposition scheme based on the extended transition state method and natural orbitals for chemical valence theory (ETS-NOCV).[12j] Calculations of ^{11}B NMR chemical shifts were performed using the NMR program contained in the ADF Package.[12k-o] Chemical shifts are referenced to H_2BNMe_2 ($\delta = 37.9$ ppm) as the experimental standard. For computational efficiency, a frozen-core approximation was used for all calculations, including the NMR chemical shifts. Run files can be found in the Supplementary Material.

Results and Discussion

Initial studies targeted the interaction of the aminoborane $H_2BN^iPr_2$ with a series of cationic half-sandwich ruthenium centres. Utilising halide abstraction chemistry and the 16-electron starting material $Cp^*Ru(PCy_3)Cl$ (**1a**), a putative 14-electron system can be accessed in situ, thereby promoting on the basis of simple electron counting considerations, a chelating κ^2 coordination mode of the aminoborane (Scheme 2). In practice, and in contrast to chemistry reported by Stradiotto and co-workers for the more electrophilic borane $[H_2BMes]_n$,[8] premixing of either $H_2BN^iPr_2$ or H_2BNCy_2 with the 16-electron ruthenium starting material **1a** in fluorobenzene leads to no change in either the ^{11}B or ^{31}P NMR spectrum. Subsequent treatment of these intensely blue coloured solutions with a single equivalent of $Na[BAr^f_4]$, however, results in an immediate colour change to bright yellow; ^{11}B and ^{31}P NMR spectroscopic analyses reveal quantitative conversion to a single complex in each case, characterised by signals at $\delta_B = 56.2$, $\delta_P = 53.3$ ppm (for $[\mathbf{2a}]^+$) and $\delta_B = 56.5$, $\delta_P = 54.4$ ppm (for $[\mathbf{3a}]^+$). In both cases, large red crystals could subsequently be obtained in ~60 % yield by layering the reaction mixture with hexanes.

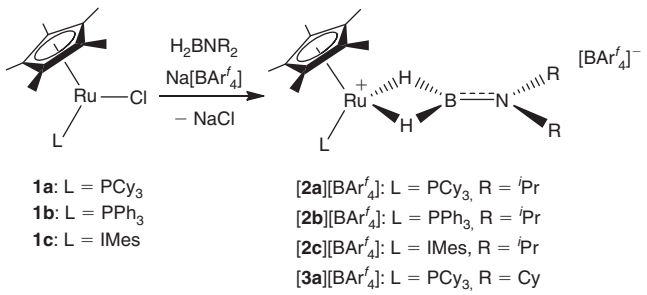

Scheme 2. Syntheses of half-sandwich ruthenium κ^2-aminoborane complexes from 16-electron $Cp^*Ru(L)Cl$ precursors.

NMR data obtained for crystalline samples support the formation of $[Cp^*Ru(PCy_3)(\kappa^2\text{-}H_2BNR_2)][BAr^f_4]$ (R = ^{i}Pr: $[\mathbf{2a}][BAr^f_4]$; R = Cy: $[\mathbf{3a}][BAr^f_4]$; Scheme 2). Thus, the respective ^1H NMR spectra feature signals associated with the Cp*, PCy_3, and $[BAr^f_4]^-$ moieties. In addition, for $[\mathbf{2a}][BAr^f_4]$ a single set of signals corresponding to the isopropyl CH (sept, $^3J_{HH} = 6.6$ Hz) and CH_3 protons (d, $^3J_{HH} = 6.6$ Hz) is observed, consistent with the equivalent N^iPr_2 isopropyl substituents expected for a symmetrically bound κ^2 complex.[5] Similar findings have been reported previously by Tang et al. in the synthesis of $[M(IMes)_2(H)_2(\kappa^2\text{-}H_2BN^iPr_2)]^+$ (M = Rh, Ir).[5b,d] Furthermore, in each case, a broad signal in the hydride region ($[\mathbf{2a}]^+$: $\delta_H = -11.21$ ppm; $[\mathbf{3a}]^+$: $\delta_H = -11.22$ ppm), which can be resolved into a doublet in the $^1H\{^{11}B\}$ spectrum ($[\mathbf{2a}]^+$: $^2J_{HP} = 15.0$ Hz; $[\mathbf{3a}]^+$: $^2J_{HP} = 14.8$ Hz), provides evidence for coordination of the aminoborane to the $[Cp^*Ru(PCy_3)]^+$ fragment in solution. By means of comparison, the corresponding data reported for the κ^2 mesitylborane complex $[Cp^*Ru(P^iPr_3)(\kappa^2\text{-}H_2BMes)]^+$ are $\delta_H = -10.3$ ppm, $^2J_{PH} = 15.0$ Hz.[8] For both $[\mathbf{2a}]^+$ and $[\mathbf{3a}]^+$, the ESI mass spectrum shows the expected $[M]^+$ envelope, with the identity of the molecular ion being confirmed by accurate mass measurements. Bulk sample purity was confirmed by elemental microanalysis and the structures of both $[\mathbf{2a}][BAr^f_4]$ and $[\mathbf{3a}][BAr^f_4]$ in the solid state were determined by X-ray crystallography (Fig. 1).

The molecular structures of both cations contain an aminoborane ligand featuring a near planar C_2NBH_2 skeleton coordinated to the metal via two B-H-M interactions. The essentially linear Ru···B–N framework [$\angle$ Ru···B–*N* = 171.6(2), 169.8(3)° for $[\mathbf{2a}]^+$ and $[\mathbf{3a}]^+$, respectively] is similar in nature to that observed for other κ^2-bound aminoborane ligands {e.g. 179.6(3)° for $[(IMes)_2Rh(H)_2(H_2BN^iPr_2)]^+$},[5b,d] and the B–N distances [1.362(3), 1.353(6) Å] are consistent with considerable π bond character [compare with 1.58 Å for the sum of the respective covalent radii and 1.380(6) Å for the B–N separation in Ph_2NBCl_2].[13,14] The Ru···B separations [1.965(3), 1.986(4) Å] are statistically identical to that reported by Sabo-Etienne and co-workers for the non-Cp system $(Cy_3P)_2Ru(H)_2(\kappa^2\text{-}H_2BN^iPr_2)$ [1.980(3) Å],[5e] but significantly shorter than that in $[CpRu(PMe_3)_2(\kappa^1\text{-}H_3B{\cdot}NMe_3)]^+$ [2.648 (3) Å],[15] presumably reflecting the presence of a three (rather than four)-coordinate boron centre and the possibility for Ru to B back-bonding. By means of further comparison, the Ru···B separation in $[Cp^*Ru(P^iPr_3)(\kappa^2\text{-}H_2BMes)]^+$ is 1.921(2) Å.[8]

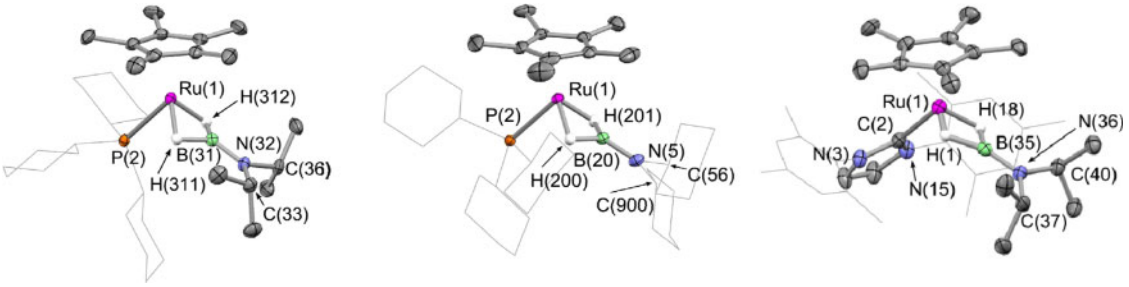

Fig. 1. Molecular structures of $[\mathbf{2a}][BAr^f_4]$ (left), $[\mathbf{3a}][BAr^f_4]$ (centre) and $[\mathbf{2c}][BAr^f_4]$ (right) as determined by X-ray crystallography. Thermal ellipsoids set at the 35 % probability level; H atoms (except metal-bound Hs) and counter-ion omitted, and Mes/Cy groups shown in wireframe format for clarity. Key bond lengths (Å) and angles (°): (for $[\mathbf{2a}]^+$) Ru(1)···B(31) 1.965(3), B(31)–N(32) 1.362(3), Ru(1)–P(1) 2.388(1), Ru(1)···B(31)–N(32) 171.6(2); (for $[\mathbf{3a}]^+$): Ru(1)···B(20) 1.986(4), B(2)–N(5) 1.353(6), Ru(1)–P(2) 2.384(1), Ru(1)···B(20)–N(5) 1.698(3); (for $[\mathbf{2c}]^+$) Ru(1)···B(35) 1.972(6), B(35)–N(36) 1.372(7), Ru(1)–C(2) 2.113(5), Ru(1)···B(31)–N(32) 170.6(5).

Variation in the ancillary two-electron donor ligand, L is also possible. Thus, the corresponding reactions in fluorobenzene of Cp*Ru(L)Cl (**1b**: L = PPh_3; **1c**: L = IMes) with $H_2BN^iPr_2$/$Na[BAr^f_4]$ yield, in each case, a κ^2-aminoborane adduct closely related to $[\mathbf{2a}]^+$ (Scheme 2). Both [Cp*Ru(PPh_3)(κ^2-$H_2BN^iPr_2$)][BAr^f_4] ($[\mathbf{2b}][BAr^f_4]$) and [Cp*Ru(IMes)(κ^2-$H_2BN^iPr_2$)][BAr^f_4] ($[\mathbf{2c}][BAr^f_4]$) have been characterised by multinuclear NMR spectroscopy and mass spectrometry, with the ^{11}B NMR spectrum of each compound featuring a broad downfield shifted resonance ($[\mathbf{2b}]^+$: $\delta_B = 57.2$ ppm; $[\mathbf{2c}]^+$: $\delta_B = 49.9$ ppm). Additionally, the corresponding ^1H NMR spectra feature Ru-H-B resonances in the expected chemical shift range ($[\mathbf{2b}]^+$: $\delta_H = -10.45$ ppm; $[\mathbf{2c}]^+$: $\delta_H = -9.71$ ppm). While $[\mathbf{2b}][BAr^f_4]$ appears to be an oil, the IMes derivative $[\mathbf{2c}][BAr^f_4]$ can be obtained as a crystalline solid allowing for (i) establishment of its bulk purity by elemental microanalysis; and (ii) structure determination by single crystal X-ray diffraction (Fig. 1). The structure of the $[\mathbf{2c}]^+$ cation is very similar to those of $[\mathbf{2a}]^+$/$[\mathbf{3a}]^+$, being based around a familiar linear Ru···B–N framework [$\angle$ Ru···B-N = 170.6(5)°] and featuring a Ru···B separation [1.972(6) Å] which is statistically identical to the two PCy_3-ligated compounds.

In the cases of half-sandwich complexes outlined above, the Ru···B contacts [1.965(3)-1.986(4) Å] fall comfortably within the sum of the respective covalent radii (2.12 Å),[14] and the ^{11}B chemical shifts (49.9 to 57.2 ppm) are also shifted significantly downfield, both with respect to the free aminoborane (35.4 ppm),[10a,b] and to cationic rhodium and iridium complexes featuring a similar κ^2-mode of ligand coordination (e.g. 35.9, 37.9 ppm for $[M(IMes)_2(H)_2(\kappa^2\text{-}H_2BN^iPr_2)]^+$, where M = Rh or Ir, respectively).[5b,d] These observations prompted us to investigate the nature of the interaction between the ruthenium centre and the aminoborane ligand in systems such as $[\mathbf{2a}]^+$ by DFT methods. Of particular interest was the extent to which the metal-borane interaction might be augmented by back-bonding from the metal into boron-centred molecular orbitals (e.g. of BH σ* or BN π* character).[5e]

While there is general agreement between the structures $[\mathbf{2a}]^+$ obtained by X-ray crystallography and DFT, several small yet significant differences are noted. Notably, the Ru···B (2.091 Å) and Ru–H (1.855 and 1.860 Å) distances are longer (by 0.126 and 0.214/0.197 Å, respectively), the B–H (1.297 and 1.299 Å) distances are shorter (by 0.037/0.036 Å), and the Ru···B-N (168.2°) angle is slightly more distorted from linear (by 3.4°) in the calculated structure. These values suggest less activated B–H bonds in the calculated structure, a hypothesis also consistent with the relatively upfield calculated ^{11}B NMR shift of 41.2 ppm (compared to 56.2 ppm measured experimentally). Previous reports imply that DFT methods tend to underestimate the strength of bonding interactions involving bridging hydrogens.[16] Consistently, re-optimising the geometry but constraining the Ru–H distances to be 1.65 Å (as in the X-ray structure) results in a structure ~5 kcal mol^{-1} higher in energy, but possessing metrics closer to those observed in the solid state [d(B–N) = 1.386, d(Ru···B) = 1.967, d(B–H) = 1.402, 1.405 Å; $\angle$(Ru···B-N) = 172.4°] and in solution ($\delta_B = 54.4$ ppm).

The binding energy for the aminoborane ligand in $[\mathbf{2a}]^+$, reflecting the difference in energy between the freely optimised complex and $[Cp^*Ru(PCy_3)]^+$/$H_2BN^iPr_2$ fragments, is calculated to be 23.6 kcal mol^{-1}. This reflects the energy required to distort the free fragments to their complex geometries (18.3 kcal mol^{-1}) and the instantaneous interaction energy (41.8 kcal mol^{-1}), the latter being the difference between steric (40.1 kcal mol^{-1}) and orbital interaction (81.9 kcal mol^{-1}) energies. In the system featuring Ru–H bond constraints, the corresponding binding energy is marginally less (18.5 kcal mol^{-1}), reflecting increases in both the distortion energy (37.3 kcal mol^{-1}) and steric energy (81.5 kcal mol^{-1}) which are not quite offset by that in the orbital interaction energy (137.3 kcal mol^{-1}). In terms of the importance of σ-donation and π-back-bonding, ETS-NOCV analyses imply that the relative energetic contributions are in the ratio of ~1 : 2 in favour of back-bonding (e.g. 1 : 2.3 for the freely optimised system; 1 : 1.8 for the Ru–H constrained system). The predominant ligand-to-metal σ-bonding interaction originates in the higher lying (out of phase) B–H bonding orbital, while the major component of metal-to-ligand π back-bonding involves the aminoborane B–N π* orbital.[5e,6a]

Despite their isoelectronic relationship with 1,1-disubstituted alkenes, the coordination chemistry of aminoboranes was first reported in the literature as late as 2010.[4,5a,b] Cations $[\mathbf{2a}\text{–}\mathbf{c}]^+$ and $[\mathbf{3a}]^+$ thus represent significant additions to a limited class of complexes featuring κ^2-aminoborane ligation – and the first such systems featuring a half-sandwich metal fragment. Such a coordination geometry contrasts with the classical 'side-on' binding mode typically observed for alkene donors, and can be rationalised by the more hydridic nature of the B–H bonds (compared with C–H), and the significantly lower energy of the B=N π system (compared with C=C).[17,18] Consistently, Alcaraz and Sabo-Etienne report an energetic preference of 14.3 kcal mol^{-1} for the 'end-on' *bis*(σ-BH) coordination geometry of H_2BNH_2 at charge neutral *bis*(phosphine)ruthenium fragments of the type $[L_2Ru(H)_2]$.[5a] Attempts to encourage coordination through the B=N π system by employing non-hydridic aminoboranes such as Me_2BNMe_2,[19] however, do not result in side-on coordination. Rather, the very weakly interacting nature of the π system is emphasised by the fact that the reaction of **1a** with $Na[BAr^f_4]$/Me_2BNMe_2 in fluorobenzene leads to the generation of the known phosphino-allyl complex $[Cp^*Ru(H)\{\kappa^2\text{-}PCy_2(C_6H_8)\}]^+$ (Scheme 3),[6b,20] presumably via multiple C–H activation within one of the cyclohexyl substituents of the putative 14-electron intermediate $[Cp^*Ru(PCy_3)]^+$.[6b] Moreover, the fact that the Me_2BNMe_2 molecule is not found to coordinate to the $[Cp^*Ru(PCy_3)]^+$ fragment is consistent with the predictions of DFT calculations which imply that dissociation is favoured by 5.4 kcal mol^{-1}.

While the dominance of the σ-borane mode of coordination of aminoboranes of the type H_2BNR_2 has thus been established, the utilisation of a 14-electron metal fragment such as $[L_2Ru(H)_2]$, $[L_2M(H)_2]^+$ (M = Rh, Ir), or $[(\eta^5\text{-}C_5R_5)Ru(L)]^+$, might be viewed as distorting the structural landscape in favour of the four-electron-donating *bis*(σ-BH) coordination mode over a possible (two-electron-donating) side-on π-bound motif. With this in mind, we have also sought to determine the intrinsic two-electron donor capabilities of aminoborane ligands, by employing 16-electron metal centres.[6a]

Two complementary synthetic strategies have been employed to target aminoborane complexes of 16-electron metal fragments (Scheme 4), namely (i) displacement of a labile ligand from an 18-electron precursor by an aminoborane (e.g. route 1, L′ = N_2); and (ii) modification of a κ^2-aminoborane complex by the assimilation of an additional two electron donor (route 2). While the former strategy has been shown to be successful in the synthesis of κ^1 complexes of H_2BNCy_2 featuring $[CpRu(PPh_3)_2]^+$ and $[CpRu(dcype)]^+$ fragments,[6a]

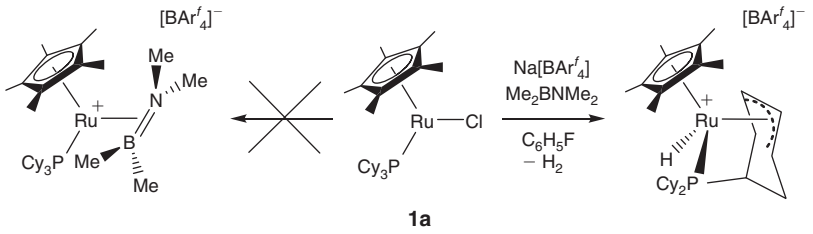

1a

Scheme 3. Reaction of **1a** with Na[BAr$^f_4$]/Me_2BNMe_2: CH activation vs borane ligation.

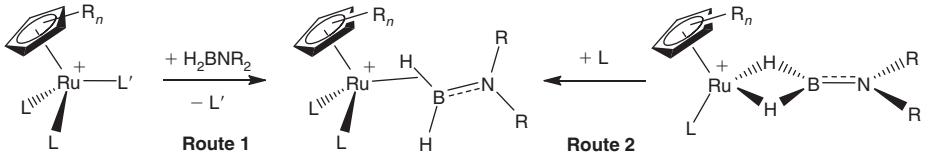

Scheme 4. Potential routes to half-sandwich ruthenium κ^1-aminoborane complexes.[6a]

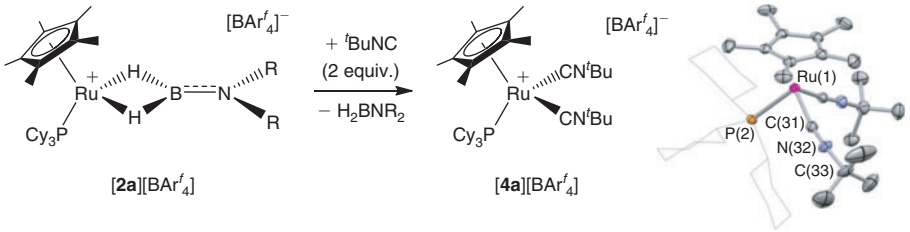

[**2a**][BAr$^f_4$] [**4a**][BAr$^f_4$]

Scheme 5. Reaction of [**2a**][BAr$^f_4$] with ^{t}BuNC; crystal structure of [**4a**][BAr$^f_4$] with H atoms and counter-ion omitted and Cy groups shown in wireframe format for clarity; thermal ellipsoids are set at the 40 % probability level.

the second route was perceived as offering a potential route to unsymmetrically ligated systems of the type [Cp*Ru($L^{[1]}$)(L^2)(κ^1-H_2BNR_2)]$^+$ via reactions of [**2a**–**c**]$^+$ or [**3a**]$^+$ with two-electron donors.

With this in mind, DFT calculations were carried out on the exemplar model system [CpRu(PMe_3)(CNMe)(H_2BNMe_2)]$^+$ with the aim of probing (i) the relative energies of different modes of aminoborane attachment (e.g. via B–H or B=N donation); and (ii) whether the presence of electronic asymmetry within the ancillary ligand set (based on the differing σ donor and π acceptor properties of the tertiary phosphine and isonitrile donors) leads to any orientational preference in the aminoborane binding. For the model κ^2 system [CpRu(PMe_3)(H_2BNMe_2)]$^+$, the *bis*(σ-BH) binding mode (42.1 kcal mol^{-1}) is significantly favoured over π-BN coordination (19.8 kcal mol^{-1}). With a mean contribution of 21 kcal mol^{-1} per bridging Ru-B-H interaction, this suggests that a single σ-BH interaction might still be favoured over the π-BN motif. Upon introducing a CNMe ligand, the ruthenium centre adopts a pseudo-tetrahedral geometry and becomes chiral, resulting in subtle differences depending on the relative orientation of the H_2BNMe_2 ligand. In the two local minima, the B–H bond is orientated either towards the phosphine or the isonitrile co-ligand (and thus is pseudo-trans to the other ligand); these rotamers have very similar binding energies (23.4 and 22.9 kcal mol^{-1}, respectively). While such a small difference (~0.5 kcal mol^{-1}) precludes significant interpretation, it is interesting that the lower energy species, with the B–H bond aligned towards the phosphine, is slightly further along the oxidative pathway (the B–H is 0.026 Å longer and the Ru–B is 0.024 Å shorter) with a larger instantaneous interaction energy to compensate for the greater distortion energy (~3.5 kcal mol^{-1}). In considering a side-on π-bound motif for H_2BNMe_2 (or indeed the isosteric/isoelectronic alkene H_2CCMe_2), the orientation in which the Me groups point away from the larger phosphorus substituent (rather than the smaller Cp ligand) is favoured on steric grounds. However, not surprisingly, the 'side-on' B=N bond binds significantly less strongly (15.9 kcal mol^{-1}) than the corresponding C=C bond (22.1 kcal mol^{-1}), or than either of the mono σ-(BH) possibilities (23.4/22.9 kcal mol^{-1}).

The reactions of [**2a**][BAr$^f_4$] with a series of neutral two-electron donor ligands were therefore probed by NMR and (in the case of ^{t}BuNC) crystallographic techniques. These studies revealed that, while [**2a**]$^+$ is unreactive towards the weaker donor THF, its reactions towards ^{t}BuNC, Ph_2CO, PMe_3, PPh_3, and PCy_3 are characterised by extrusion of the borane fragment. The related reaction between [**2a**]$^+$ and [PPh_4]Cl results in regeneration of the intensely blue coloured starting material Cp*Ru(PCy_3)Cl (**1a**) and $H_2BN^iPr_2$. In the case of the reaction with ^{t}BuNC, extrusion of the borane was not only confirmed by the identification (via multinuclear NMR) of the free borane $H_2BN^iPr_2$, but also by the isolation and structural characterisation of the metal-containing product [Cp*Ru(PCy_3)($CN^tBu)_2$][BAr$^f_4$] ([**4a**][BAr$^f_4$]) (Scheme 5). Although the quality of the structure solution is not sufficient to justify discussion of metrics, atomic connectivity and the formation of the 18-electron *bis*(isonitrile) cation are thus confirmed.

While the formation of [**4a**][BAr$^f_4$] from [**2a**][BAr$^f_4$] implies a 2 : 1 stoichiometry for isonitrile uptake, studies carried out with a molar ratio of 1 : 1 give no indication of the formation of

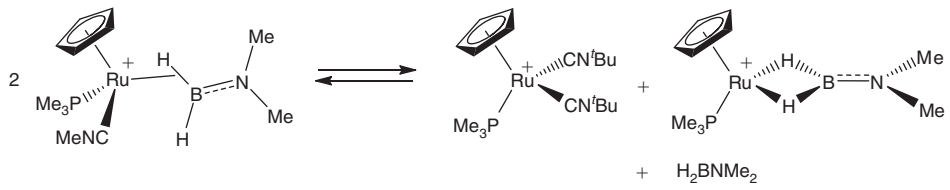

Scheme 6. Ligand redistribution in the model κ^1-aminoborane complex $[CpRu(PMe_3)(CNMe)(\kappa^1\text{-}H_2BNMe_2)]^+$ probed by DFT methods.

the κ^1 complex $[Cp^*Ru(PCy_3)(CN^tBu)(\kappa^1\text{-}H_2BN^iPr_2)]^+$. Moreover, in-depth analysis of the thermodynamics of the related model system $[CpRu(PMe_3)(CNMe)(\kappa^1\text{-}H_2BNMe_2)]^+$ by DFT methods implies that the ligand redistribution reaction represented by Scheme 6 is exergonic by 7.6 kcal mol^{-1}. As such, the implication for isonitrile systems at least, is that κ^1 systems are unlikely to be accessible from related κ^2 complexes via a ligand addition protocol, being clearly disfavoured with respect to more symmetrically substituted systems.

Conclusions

Cationic half-sandwich ruthenium complexes featuring κ^2-bound aminoborane ligands can readily be accessed from 16-electron precursors via chloride abstraction in the presence of H_2BNR_2 ($R = {}^i$Pr, Cy). Low-field ^{11}B NMR shifts for the coordinated aminoborane fragment, together with short Ru···B contacts (of the order of 1.97 Å) imply a relatively tightly bound borane ligand, a finding which is given further credence by the results of DFT studies (e.g. bond dissociation energies in the range 24 kcal mol^{-1}). Reactivity-wise κ^2 systems of this type, while potentially offering a versatile route to asymmetric κ^1 systems, in fact undergo borane extrusion even in the presence of a single equivalent of added ligand.

Supplementary Material

Full details of DFT calculations (optimised geometries and run files) and CIFs for all X-ray structures are available on the Journal's website.

Acknowledgements

We thank the EPSRC for a doctoral training grant studentship and post-doctoral support (DAA), and NSERC for a post-doctoral fellowship (JIB).

References

[1] For recent reviews of BN-containing materials see, for example:
(a) T. J. Clark, K. Lee, I. Manners, *Chem. – Eur. J.* **2006**, *12*, 8634. doi:10.1002/CHEM.200600981
(b) T. B. Marder, *Angew. Chem., Int. Ed.* **2007**, *46*, 8116. doi:10.1002/ANIE.200703150
(c) F. H. Stephens, V. Pons, R. T. Baker, *Dalton Trans.* **2007**, 2613. doi:10.1039/B703053C
(d) C. W. Hamilton, R. T. Baker, A. Staubitz, I. Manners, *Chem. Soc. Rev.* **2009**, *38*, 279. doi:10.1039/B800312M
(e) N. C. Smythe, J. C. Gordon, *Eur. J. Inorg. Chem.* **2010**, 509. doi:10.1002/EJIC.200900932
(f) A. Staubitz, A. P. M. Robertson, M. E. Sloan, I. Manners, *Chem. Rev.* **2010**, *110*, 4023. doi:10.1021/CR100105A
(g) A. Staubitz, A. P. M. Robertson, I. Manners, *Chem. Rev.* **2010**, *110*, 4079. doi:10.1021/CR100088B

[2] (a) For early examples of the metal-catalysed formation of poly (methylaminoborane) see: A. Staubitz, A. P. Soto, I. Manners, *Angew. Chem. Int. Ed.* **2008**, *47*, 6212. doi:10.1002/ANIE.200801197
(b) A. Staubitz, M. E. Sloan, A. P. M. Robertson, A. Friedrich, S. Schneider, P. J. Gates, J. S. A. D. Guenne, I. Manners, *J. Am. Chem. Soc.* **2010**, *132*, 13332. doi:10.1021/JA104607Y

[3] (a) For recent reviews of σ-borane complexes see, for example: R. N. Perutz, S. Sabo-Etienne, *Angew. Chem. Int. Ed.* **2007**, *46*, 2578. doi:10.1002/ANIE.200603224
(b) Z. Lin, *Struct. Bond.* **2008**, *130*, 123. doi:10.1007/430_2007_074
(c) G. Alcaraz, S. Sabo-Etienne, *Coord. Chem. Rev.* **2008**, *252*, 2395. doi:10.1016/J.CCR.2008.02.006
(d) K. K. Pandey, *Coord. Chem. Rev.* **2009**, *253*, 37. doi:10.1016/J.CCR.2007.11.026
(e) G. Alcaraz, M. Grellier, S. Sabo-Etienne, *Acc. Chem. Res.* **2009**, *42*, 1640. doi:10.1021/AR900091A
(f) G. Alcaraz, S. Sabo-Etienne, *Angew. Chem. Int. Ed.* **2010**, *49*, 7170. doi:10.1002/ANIE.201000898

[4] For an early spectroscopic report examining aminoborane interactions with transition metals see: G. Schmid, *Chem. Ber.* **1970**, *103*, 528. doi:10.1002/CBER.19701030222

[5] (a) For previous reports of κ^2-coordinated aminoboranes, see: G. Alcaraz, L. Vendier, E. Clot, S. Sabo-Etienne, *Angew. Chem. Int. Ed.* **2010**, *49*, 918. doi:10.1002/ANIE.200905970
(b) C. Y. Tang, A. L. Thompson, S. Aldridge, *Angew. Chem. Int. Ed.* **2010**, *49*, 921. doi:10.1002/ANIE.200906171
(c) M. A. Esteruelas, F. J. Fernandez-Alvarez, A. M. Lopez, M. Mora, E. Onate, *J. Am. Chem. Soc.* **2010**, *132*, 5600. doi:10.1021/JA101806X
(d) C. Y. Tang, A. L. Thompson, S. Aldridge, *J. Am. Chem. Soc.* **2010**, *132*, 10578. doi:10.1021/JA1043787
(e) G. Alcaraz, A. B. Chaplin, C. J. Stevens, E. Clot, L. Vendier, A. S. Weller, S. Sabo-Etienne, *Organometallics* **2010**, *29*, 5591. doi:10.1021/OM1004995
(f) C. J. Stevens, R. Dallanegra, A. B. Chaplin, A. S. Weller, S. A. Macgregor, B. Ward, D. McKay, G. Alcaraz, S. Sabo-Etienne, *Chem. – Eur. J.* **2011**, *17*, 3011. doi:10.1002/CHEM.201002517
(g) G. Bénac-Lestrille, U. Helmstedt, L. Vendier, G. Alcaraz, E. Clot, S. Sabo-Etienne, *Inorg. Chem.* **2011**, *50*, 11039. doi:10.1021/IC201573Q
(h) C. Y. Tang, N. Phillips, J. I. Bates, A. L. Thompson, M. J. Gutmann, S. Aldridge, *Chem. Commun.* **2012**, *48*, 8096. doi:10.1039/C2CC33361A
(i) C. Y. Tang, N. Phillips, M. J. Kelly, S. Aldridge, *Chem. Commun.* **2012**, *48*, 11999. doi:10.1039/C2CC35947B

[6] (a) For κ^1-coordinated aminoboranes, see: D. Vidovic, D. A. Addy, T. Krämer, J. McGrady, S. Aldridge, *J. Am. Chem. Soc.* **2011**, *133*, 8494. doi:10.1021/JA203051D
(b) See also: D. A. Addy, J. I. Bates, M. J. Kelly, I. M. Riddlestone, S. Aldridge, *Organometallics* **2013**, *32*, 1583 which contains a preliminary report of part of this work (spectroscopic data for compound [**2a**][BAr$^f_4$]).

[7] G. Alcaraz, E. Clot, U. Helmstedt, L. Vendier, S. Sabo-Etienne, *J. Am. Chem. Soc.* **2007**, *129*, 8704. doi:10.1021/JA0733538

[8] (a) K. D. Hesp, M. A. Rankin, R. McDonald, M. Stradiotto, *Inorg. Chem.* **2008**, *47*, 7471. doi:10.1021/IC801300M
(b) K. D. Hesp, F. O. Kannemann, M. A. Rankin, R. McDonald, M. J. Ferguson, M. Stradiotto, *Inorg. Chem.* **2011**, *50*, 2431. doi:10.1021/IC1022328

[9] (a) For other examples of ruthenium σ-borane complexes see: V. Montiel-Palma, M. Lumbierres, B. Donnadieu, S. Sabo-Etienne, B. Chaudret, *J. Am. Chem. Soc.* **2002**, *124*, 5624. doi:10.1021/JA017429Q
(b) S. Lachaize, K. Essalah, V. Montiel-Palma, L. Vendier, B. Chaudret, J.-C. Barthelat, S. Sabo-Etienne, *Organometallics* **2005**, *24*, 2935. doi:10.1021/OM050276L

(c) G. Alcaraz, U. Helmstedt, E. Clot, L. Vendier, S. Sabo-Etienne, *J. Am. Chem. Soc.* **2008**, *130*, 12878. doi:10.1021/JA805164N
(d) Y. Gloaguen, G. Alcaraz, L. Vendier, S. Sabo-Etienne, *J. Organomet. Chem.* **2009**, *694*, 2839. doi:10.1016/J.JORGANCHEM.2009.03.020
(e) M. C. MacInnis, R. McDonald, M. J. Ferguson, S. Tobisch, L. Turculet, *J. Am. Chem. Soc.* **2011**, *133*, 13622. doi:10.1021/JA204935X
(f) Y. Gloaguen, G. Alcaraz, A. S. Petit, E. Clot, Y. Coppel, L. Vendier, S. Sabo-Etienne, *J. Am. Chem. Soc.* **2011**, *133*, 17232. doi:10.1021/JA203828R
(g) See also: S. Bontemps, L. Vendier, S. Sabo-Etienne, *Angew. Chem. Int. Ed.* **2012**, *51*, 1671. doi:10.1002/ANIE.201107352

[10] (a) $H_2BN^iPr_2$: C. A. Jaska, K. Temple, A. J. Lough, I. Manners, *J. Am. Chem. Soc.* **2003**, *125*, 9424. doi:10.1021/JA030160L
(b) H_2BNCy_2: L. Euzenat, D. Horhant, Y. Ribourdouille, C. Duriez, G. Alcaraz, M. Vaultier, *Chem. Commun.* **2003**, 2280. doi:10.1039/B306874A
(c) Cp*Ru(PCy_3)Cl: T. Arliguie, C. Border, B. Chaudret, J. Devillers, R. Poilblanc, *Organometallics* **1989**, *8*, 1308. doi:10.1021/OM00107A029
(d) Cp*Ru(PPh_3)Cl: T. J. Johnson, K. Folting, W. E. Streib, J. D. Martin, J. C. Huffman, S. A. Jackson, O. Eisenstein, K. G. Caulton, *Inorg. Chem.* **1995**, *34*, 488. doi:10.1021/IC00106A010
(e) Cp*Ru(IMes)Cl: W. Baratta, W. A. Herrmann, P. Rigo, J. Schwarz, *J. Organomet. Chem.* **2000**, *593-594*, 489. doi:10.1016/S0022-328X(99)00435-0
(f) Na[BAr^f_4]: D. L. Reger, T. D. Wright, C. A. Little, J. J. S. Lamba, M. D. Smith, *Inorg. Chem.* **2001**, *40*, 3810. doi:10.1021/IC0100121

[11] (a) J. Cosier, A. M. Glazer, *J. Appl. Cryst.* **1986**, *19*, 105. doi:10.1107/S0021889886089835
(b) Z. Otwinowski, W. Minor, in *Methods in Enzymology* (Eds C. W. Carter, R. M. Sweet) **1996**, Vol. 276, pp. 307–332 (Academic Press: New York, NY).
(c) A. Altomare, G. Cascarano, C. Giacovazzo, A. Guagliardi, M. C. Burla, G. Polidori, M. Camalli, *J. Appl. Cryst.* **1994**, *27*, 435.
(d) P. W. Betteridge, J. R. Carruthers, R. I. Cooper, J. Prout, D. J. Watkin, *J. Appl. Cryst.* **2003**, *36*, 1487. doi:10.1107/S0021889803021800

[12] (a) G. te Velde, F. M. Bickelhaupt, S. J. A. van Gisbergen, C. Fonseca Guerra, E. J. Baerends, J. G. Snijders, T. Ziegler, *J. Comput. Chem.* **2001**, *22*, 931. doi:10.1002/JCC.1056
(b) C. Fonseca Guerra, J. G. Snijders, G. te Velde, E. J. Baerends, *Theor. Chem. Acc.* **1998**, *99*, 391.
(c) E. J. Baerends, T. Ziegler, J. Autschbach, D. Bashford, A. Bérces, F. M. Bickelhaupt, C. Bo, P. M. Boerrigter, L. Cavallo, D. P. Chong, L. Deng, R. M. Dickson, D. E. Ellis, M. van Faassen, L. Fan, T. H. Fischer, C. Fonseca Guerra, A. Ghysels, A. Giammona, S. J. A. van Gisbergen, A. W. Götz, J. A. Groeneveld, O. V. Gritsenko, M. Grüning, S. Gusarov, F. E. Harris, P. van den Hoek, C. R. Jacob, H. Jacobsen, L. Jensen, J. W. Kaminski, G. van Kessel, F. Kootstra, A. Kovalenko, M. V. Krykunov, E. van Lenthe, D. A. McCormack, A. Michalak, M. Mitoraj, J. Neugebauer, V. P. Nicu, L. Noodleman, V. P. Osinga, S. Patchkovskii, P. H. T. Philipsen, D. Post, C. C. Pye, W. Ravenek, J. I. Rodríguez, P. Ros, P. R. T. Schipper, G. Schreckenbach, J. S. Seldenthuis, M. Seth, J. G. Snijders, M. Solà, M. Swart, D. Swerhone, G. te Velde, P. Vernooijs, L. Versluis, L. Visscher, O. Visser, F. Wang, T. A. Wesolowski, E. M. van Wezenbeek, G. Wiesenekker, S. K. Wolff, T. K. Woo, A. L. Yakovlev, *ADF2012* **2012** (SCM, Theoretical Chemistry, Vrije Universiteit: Amsterdam). Available at http://www.scm.com (see Supplementary Material for full citation).
(d) A. D. Becke, *Phys. Rev. A* **1988**, *38*, 3098. doi:10.1103/PHYSREVA.38.3098
(e) J. P. Perdew, *Phys. Rev. B* **1986**, *33*, 8822. doi:10.1103/PHYSREVB.33.8822
(f) J. G. Snijders, P. Vernooijs, E. J. Baerends, *At. Data Nucl. Data Tables* **1981**, *26*, 483. doi:10.1016/0092-640X(81)90004-8
(g) A. Rosa, A. W. Ehlers, E. J. Baerends, J. G. Snijders, G. te Velde, *J. Phys. Chem.* **1996**, *100*, 5690. doi:10.1021/JP953381P
(h) S. F. Boys, F. Bernardi, *Mol. Phys.* **1970**, *19*, 553. doi:10.1080/00268977000101561
(i) T. Clark, *A Handbook of Computational Chemistry* **1985** (Wiley: New York, NY).
(j) M. Mitoraj, A. Michalak, T. Ziegler, *J. Chem. Theory Comput.* **2009**, *5*, 962. doi:10.1021/CT800503D
(k) G. Schreckenbach, T. Ziegler, *J. Phys. Chem.* **1995**, *99*, 606. doi:10.1021/J100002A024
(l) G. Schreckenbach, T. Ziegler, *Int. J. Quantum Chem.* **1996**, *60*, 753. doi:10.1002/(SICI)1097-461X(1996)60:3<753::AID-QUA4>3.0.CO;2-W
(m) G. Schreckenbach, T. Ziegler, *Int. J. Quantum Chem.* **1997**, *61*, 899. doi:10.1002/(SICI)1097-461X(1997)61:6<899::AID-QUA3>3.0.CO;2-R
(n) S. K. Wolff, T. Ziegler, *J. Chem. Phys.* **1998**, *109*, 895. doi:10.1063/1.476630
(o) S. K. Wolff, T. Ziegler, E. van Lenthe, E. J. Baerends, *J. Chem. Phys.* **1999**, *110*, 7689. doi:10.1063/1.478680

[13] F. Zettler, H. Hess, *Chem. Ber.* **1975**, *108*, 2269. doi:10.1002/CBER.19751080714

[14] B. Cordero, V. Gómez, A. E. Platero-Prats, M. Revés, J. Echeverría, E. Cremandes, F. Barrigán, S. Alvarez, *Dalton Trans.* **2008**, 2832. doi:10.1039/B801115J

[15] Y. Kawano, M. Hashiva, M. Shimoi, *Organometallics* **2006**, *25*, 4420. doi:10.1021/OM0604324

[16] B. G. Willis, K. F. Jensen, *J. Phys. Chem. A* **1998**, *102*, 2613. doi:10.1021/JP9800012

[17] For an example of 'side-on' binding of a phosphine borane at a late transition metal centre, see: A. Amgoune, S. Ladeira, K. Miqueu, D. Bourissou, *J. Am. Chem. Soc.* **2012**, *134*, 6560. doi:10.1021/JA301929N

[18] N. P. C. Westwood, N. H. Werstiuk, *J. Am. Chem. Soc.* **1986**, *108*, 891. doi:10.1021/JA00265A007

[19] C. E. Erickson, F. C. Gunderloy, Jr, *J. Org. Chem.* **1959**, *24*, 1161. doi:10.1021/JO01090A628

[20] T. Arliguie, B. Chaudret, F. A. Jalon, A. Otero, J. A. Lopez, F. J. Lahoz, *Organometallics* **1991**, *10*, 1888. doi:10.1021/OM00052A038